Supporting Information

Atkins et al. 10.1073/pnas.1412372111

SI Text

Identification of Remodeling by Morphology. Secondary osteons are markers of remodeling, thus present in locations of previous damage in cases where remodeling is damage driven: During remodeling, the shape and location of a resorption cavity dug by osteoclasts (and therefore the shape of the future secondary osteon, which osteoblasts will create inside it) relate only to the area of tissue in need of repair (1). In cross-section, newly created secondary osteons appear superimposed over any preexisting background tissue, be it primary (unremodeled) or previously remodeled (e.g., a field of secondary osteons) (Fig. 1 *C* and *D*) (2). The time-staggered activity of osteoclasts and osteoblasts and the fact that remodeling may occur in many different locations in the skeleton simultaneously means that a single cross-section of bone can provide a temporal snapshot of multiple stages of remodeling (Fig. 1*A*) and because remodeling is an ongoing process, many regions bear evidence of multiple "generations" of localized repair (Fig. 1 *C* and *D*). We assert that morphological demonstration of remodeling is only definitive when osteons are seen to be "overlapping" other osteons, because osteons can also exist in unremodeled tissue (primary osteons, that form de novo around blood vessels in developing bone and may occur in close proximity to one another) (3, 4). This definition of remodeling is stricter than has been used by other authors describing fish bone structure; however, purely morphological criteria for distinguishing remodeling are particularly necessary for fishes, because little information exists on their in vivo skeletal physiology and such data are exceptionally difficult to gather for many species because of their anatomy and ecology (e.g., very large or very small body sizes, pelagic oceanic habitat).

Previous Mention of Remodeling in Fish Bone. Although some previous studies have cited evidence for remodeling in fish bone, we believe most are reporting cases of what should be more strictly called "modeling" in the terminology of tetrapod bone biology. Both modeling and remodeling processes make use of osteoclasts and osteoblasts to erode and lay down bone, respectively; however, the time sequences of these processes and their end results are quite different. Modeling is effectively a bone reshaping/resizing tool, with osteoclasts and osteoblasts working in separate locations at the same time, typically on free surfaces (e.g., the periosteal or endosteal surfaces of cortical bone). The coordinated effort of the cells results in local shape change, for instance by increasing or decreasing the thickness of the cortex, and is thus vital to a bone's growth or reshaping in response to altered loading conditions. Remodeling, however, is a "replacement" process, with osteoclasts and osteoblasts working successively in the same area: First osteoclasts remove a small packet of defective tissue and then osteoblasts replace it with new bone. This results in effectively no net change in material but, as described in the body of the paper, replaces existing damaged tissue with a new osteonal structure, comprised of undamaged bone material.

Previous studies said to describe remodeling in fishes typically either detailed processes that involve reshaping of bones as a response to load or during growth (e.g., refs. 5–8) or depicted osteonal tissues with equivocal morphologies, that we feel cannot be distinguished from primary tissue (e.g., figure 2 of ref. 9; figure 1 of ref. 10; figure 3 of ref. 11; and figure 2 d, l, and s of ref. 12; see also a list of studies deemed to confuse primary and secondary osteons on page 330 of ref. 13). Regardless of whether previous examples of osteonal tissues in fishes are interpreted as primary or secondary bone, it can be said that secondary osteons in fishes have never been shown in a microscopy image in densities approaching those of large adult mammals (e.g., Fig. 1*D*).

Beyond our current data, there are two reports that we believe may depict true secondary osteonal structures in fish bone: a line-drawing of the cross-sectional anatomy of the rostrum of the swordfish, *Xiphias gladius* (Xiphiidae; figure 2c of ref. 14), depicting morphologies similar to those we show here for swordfish and other billfishes (e.g., similar to Fig. 3*A*), and a light microscopy image (figure 22 of ref. 15) of a ground section of the caudal vertebra of *Trachurus mediterraneus* (Carangidae, together with billfishes in the Carangiformes, a clade sister to the flatfishes, Pleuronectiformes; refs. 16 and 17), albeit exhibiting a seemingly much lower density of secondary osteons than we observe in the billfishes. Additionally, figure 3 of ref. 10, figure 27 of ref. 15, and ref. 3 contributed polarized light images of *Xiphias* vertebrae and rostrum, respectively, as demonstrations of remodeling; however, whereas these works clearly demonstrate a high degree of structure in the bone tissue, the features shown are difficult to discern and therefore evaluate. De Ricqlès et al. (figure 21 of ref. 15) and Meunier (figure 1d of ref. 12) separately depict sole pairs of partially overlapping osteons in the dorsal fin rays of *Lethrinus nebulosus*, an anosteocytic percamorph fish, less closely related to billfishes; however, the magnification of these images is too high to allow one to determine whether this potential remodeling example represents a general trend or is a comparatively rare occurrence. Oddly, although osteocytic fishes should have all of the cellular components believed necessary to actuate and effect remodeling in mammals, we have found no convincing published demonstration of remodeling in osteocytic fish bone. Figure 1 in Amprino and Godina (10) illustrates a relatively dense osteonal structure in the vertebrae of *Euthynnus alleteratus* (a member of the Thunnidae, one of the few examples of osteocytic bone within the otherwise anosteocytic Acanthopterygii; refs. 11, 18, and 19); however, with no obvious osteonal overlaps, it is difficult to say whether these are secondary osteons, but the presence of osteocytes and the high level of swimming performance among members of the Thunnidae suggest remodeling is likely to be essential for their skeleton.

In summary, currently the strongest support for remodeling in fish bone comes from anosteocytic species, specifically jacks and billfishes (this study; refs. 14 and 15). A thorough examination of the bone of the Scombriformes, a clade which is believed to include both anosteocytic and osteocytic species (11, 18, 19), and additional members of the Carangiformes is warranted, to clarify how widespread remodeling is among acanthopterygian fishes with active lifestyles and in clades closely related to billfishes.

Evidence Linking Remodeling to Microdamage in Mammals. As the need for remodeling in tetrapods is often dictated by the accumulation of local microdamage (20), evidence of remodeling — quantified, for example, in terms of size and shape of secondary osteons and their density (number in a unit area)— can provide indication of the location and vigor of tissue use and damage, both within a given bone and across the bones of different individuals and species (although remodeling can occur for reasons other than damage removal; ref. 20). For example, remodeling seems to be rare in bones of very small animals, whose bones are unlikely to experience high loading demands (e.g., those of small rodents) or in bones that do not exist for sufficient time to create

significant damage (e.g., rodents with short life spans or seasonal bones like antler) (21–27). At the other extreme, bones of mature, larger mammals (e.g., humans, cows and horses) show dense populations of secondary osteons, which may occupy the entire cortex of a bone or, in cases of more limited loading regimes, be localized to specific areas (e.g., the region of muscle attachment in Fig. 1*A*) (2, 28–30). Beyond these correlations of snapshots of morphology with animal physiology, the direct association of remodeling morphology with use and microdamage has been demonstrated in vivo for mammals, by comparison of exercised animals or bones loaded in fatigue with controls, supporting our extrapolation of the presence of secondary osteons to loading history (1, 31–34).

SI Methods

Animals and Samples. We collected the bills of five species of billfishes: blue marlin (*Makaira nigricans*) ($n = 2$), white marlin (*Kajikia albida*) ($n = 1$), sailfish (*Istiophorus albicans*) ($n = 1$), shortbill spearfish (*Tetrapturus angustirostris*) ($n = 3$), and swordfish (*Xiphias gladius*) ($n = 2$). All samples were collected along the Gulf of Mexico from participants of fishing competitions. Specimens were wrapped in plastic and frozen until sections were cut. Transverse sections and cubes were cut from several locations (from base to tip: 25, 50, 75, and 95% along the length of the bill) by using a water-cooled rotary diamond saw (Isomet low speed saw; Buhler), then ground with emery paper of increasing grit and polished with 3-μm and 1-μm diamond suspension.

Light Microscopy. Transverse sections from the 25, 50, 75, and 95% locations were ground and polished, then examined by a reflected-light microscope (Olympus BX 51 microscope). Images were captured by using a high-resolution camera, and between 250 and 1,300 individual images of each slice were stitched together by using Microsoft composition editor (Microsoft ICE), to create a panoramic view.

Polarized Light Microscopy. Transverse sections from the 75% location were ground to a final thickness of 50 μm and imaged by a linear polarized light microscope (Nikon Eclipse E600-POL).

Scanning Electron Microscopy. Electron microscopy images of transverse sections of the 75% location where obtained for three species: swordfish, blue marlin, and shortbill with a JEOL scanning electron microscope (JSM-5410 LV) with an accelerating voltage of 20 kV, at working distance of 20 mm, in low vacuum (LV) mode and using a backscattered electron image detector.

Medical CT Scanning, Micro CT Scanning, and Quantification of Canal Networks. Heads from all five billfish species were CT scanned with a 64-slice Aquilon Toshiba scanner (Toshiba American Medical Systems) with slice thickness ranging from 0.75 to 1.0 mm; skulls were volume-rendered in Mimics software (Materialise HQ).

Cubes of 2 × 2 × 2 mm were prepared from the densest compact bone in the 95% location of the bill of a blue marlin and from the middiaphysis of a third metacarpal bone of a horse and scanned by using a microcomputed tomography scanner (1172 scanner, SkyScan). The X-ray source was set at 80 kVp and 124 μA. A total of 1,200 projections were acquired over an angular range of 180° with an isotropic voxel size of 2.4 μm, integration time of 1,250 ms, and a 0.5-mm Aluminum filter. Canal networks were volume-rendered for anatomical investigation by using Drishti software (sf.anu.edu.au/Vizlab/drishti).

To calculate the distribution of the orientations of canals, binarized CT data of the Haversian canal system were skeletonized by using a MATLAB routine developed to analyze osteocyte lacunar-canalicular networks (35). For a quantitative analysis of orientation, each segment between canal intersections was smoothed (36) and the angle, θ, with respect to the long axis of the bone was calculated for every piecewise segment of 0.5 μm length, from 0° for the axial (z) direction to 90° for dorsal (x)/medial (y) directions (Fig. 4*C*). These angular data were visualized by color-coding the skeletonized canals in three dimensions using MayaVi (37) and then summarized in a frequency histogram of canal segment angles (Fig. 4*C*).

Mechanical Testing. Cortical bone beams were obtained from representatives of each of the five billfish species (from the 75% location, two to five samples per species), horse (*Equus caballus*: third metatarsal bone, three samples), human (*Homo sapiens*: femora and metatarsi, 13 samples), carp (*Cyprinus carpio*: opercula, six samples), and tilapia (*Oreochromis aureus*: opercula, 17 samples) for three-point bending tests. The beams were 18–22 mm long, 2 mm wide and 0.5–1.0 mm thick. The billfish beams were cut from a dense part of the bill, from the midoperculum for carp and tilapia, and from the cortical midshaft of human and horse bones. All beams were tested within a custom-built micromechanical-testing device within a saline-filled testing chamber. Load-deformation data were collected and converted to stress and strain by using beam theory. At the end of mechanical testing, the beams were scanned at high resolution by microCT (1174 scanner, SkyScan) to determine their bone mineral density, calibrated with two phantoms of known mineral density (0.25 g/cm^3 and 0.75 g/cm^3) supplied by SkyScan and scanned under exactly the same conditions as the bone specimens.

Cubes of 2 × 2 × 2 mm were prepared from the densest compact bone in the 75% location of the bills of all billfishes. Three orthogonal surfaces of the cubes were carefully polished for light microscopy studies, then tested in compression in all three orthogonal anatomical orientations (Fig. 4), using a materials testing machine (Instron 3345 single column device; Instron), remaining well within the elastic limits of the material.

1. Mori S, Burr DB (1993) Increased intracortical remodeling following fatigue damage. *Bone* 14(2):103–109.
2. Gibson VA, Stover SM, Gibeling JC, Hazelwood SJ, Martin RB (2006) Osteonal effects on elastic modulus and fatigue life in equine bone. *J Biomech* 39(2):217–225.
3. Castanet J, de Ricqlès A (1986) Sur la relativité de la notion d'ostéones primaires et secondaires et de tissus osseux primaire et secondaire en général [On the relativity of the concept of primary and secondary osteons, and of primary and secondary bone tissues in general]. *Annales de sciences naturelles (Biologie animale, zoologie)* 8:103–109.
4. Currey JD (2002) *Bones* (Princeton Univ Press, Princeton, NJ), pp 436.
5. Huysseune A, Sire JY, Meunier FJ (1994) Comparative study of lower pharyngeal jaw structure in two phenotypes of *Astatoreochromis alluaudi* (Teleostei: Cichlidae). *J Morphol* 221(1):25–43.
6. Nemoto Y, Higuchi K, Baba O, Kudo A, Takano Y (2007) Multinucleate osteoclasts in medaka as evidence of active bone remodeling. *Bone* 40(2):399–408.
7. Witten PE, Hall BK (2003) Seasonal changes in the lower jaw skeleton in male Atlantic salmon (*Salmo salar L.*): Remodelling and regression of the kype after spawning. *J Anat* 203(5):435–450.
8. Witten PE, Hansen A, Hall BK (2001) Features of mono- and multinucleated bone resorbing cells of the zebrafish *Danio rerio* and their contribution to skeletal development, remodeling, and growth. *J Morphol* 250(3):197–207.
9. Wisniowski P (1935) Über den Aufbau der Knochen des Innenskellets bei Cypriniden. *Anat Anz* 80:161–204.
10. Amprino R, Godina G (1955) Osservazioni sui rinnovamento strutturale dell'osso in Pesci Teleostei [Observations on structural remodeling of bones of teleost fish]. *Publicazioni della stazione della zoologia di Napoli* 28:62–71.
11. Huysseune A, Meunier FJ (1992) The concept of bone tissue in Osteichthyes. *Neth J Zool* 42(2-3):445–458.
12. Meunier FJ (2011) The Osteichtyes, from the Paleozoic to the extant time, through histology and palaeohistology of bony tissues. *C R Palevol* 10(5-6):347–355.
13. Ørvig T (1951) Histologic studies of Placoderms and fossil Elasmobranchs. I: The endoskeleton, with remarks on the hard tissues of lower vertebrates in general. *Ark Zool* 2:322–469.
14. Poplin C, de Ricqlès A (1976) Anatomie comparée: Quelques particularités anatomiques et histologiques du rostre de l'Espadon (*Xiphias gladius* L.) [Comparative

anatomy: Some peculiar aspects of the anatomy and histology of the rostrum of swordfish (*Xiphias gladius* L)]. C.R. *Acad. Sc. Paris* 282:1105–1108.
15. de Ricqlès A, Meunier FJ, Castanet J Francillon-Vieillot H (1991) *Comparative Microstructure of Bone* (CRC, Boca Raton, FL).
16. Near TJ, et al. (2013) Phylogeny and tempo of diversification in the superradiation of spiny-rayed fishes. *Proc Natl Acad Sci USA* 110(31):12738–12743.
17. Little AG, Lougheed SC, Moyes CD (2010) Evolutionary affinity of billfishes (Xiphiidae and Istiophoridae) and flatfishes (Plueronectiformes): Independent and trans-subordinal origins of endothermy in teleost fishes. *Mol Phylogenet Evol* 56(3):897–904.
18. Kölliker A (1859) On the different types in the microscopic structure of the skeleton of osseous fishes. *Proc Biol Sci* 9:656–688.
19. Kranenbarg S, van Cleynenbreugel T, Schipper H, van Leeuwen J (2005) Adaptive bone formation in acellular vertebrae of sea bass (*Dicentrarchus labrax* L.). *J Exp Biol* 208(Pt 18):3493–3502.
20. Burr DB (2002) Targeted and nontargeted remodeling. *Bone* 30(1):2–4.
21. Enlow DH (1962) Functions of the Haversian system. *Am J Anat* 110:269–305.
22. Erben RG (1997) Embedding of bone samples in methylmethacrylate: An improved method suitable for bone histomorphometry, histochemistry, and immunohistochemistry. *J Histochem Cytochem* 45(2):307–313.
23. Foote JS (1915) A contribution to the comparative histology of the femur. *Smithsonian Contribution to Knowledge* 35(3):1–684.
24. Jowsey J (1966) Studies of Haversian systems in man and some animals. *J Anat* 100(Pt 4):857–864.
25. Krauss S, Wagermaier W, Estevez JA, Currey JD, Fratzl P (2011) Tubular frameworks guiding orderly bone formation in the antler of the red deer (*Cervus elaphus*). *J Struct Biol* 175(3):457–464.
26. Martiniaková M, Grosskopf B, Vondráková M, Omelka R, Fabiš M (2005) Observation of the microstructure of rat cortical bone tissue. *Scr Med (Brno)* 78:45–50.
27. Ruth EB (1953) Bone studies. II. An experimental study of the Haversian-type vascular channels. *Am J Anat* 93(3):429–455.
28. Skedros JG, Mason MW, Nelson MC, Bloebaum RD (1996) Evidence of structural and material adaptation to specific strain features in cortical bone. *Anat Rec* 246(1):47–63.
29. Skedros JG, Sorenson SM, Jenson NH (2007) Are distributions of secondary osteon variants useful for interpreting load history in mammalian bones? *Cells Tissues Organs* 185(4):285–307.
30. Skedros JG, Sybrowsky CL, Parry TR, Bloebaum RD (2003) Regional differences in cortical bone organization and microdamage prevalence in Rocky Mountain mule deer. *Anat Rec A Discov Mol Cell Evol Biol* 274(1):837–850.
31. Bouvier M, Hylander WL (1996) The mechanical or metabolic function of secondary osteonal bone in the monkey *Macaca fascicularis*. *Arch Oral Biol* 41(10):941–950.
32. Lanyon LE, Goodship AE, Pye CJ, MacFie JH (1982) Mechanically adaptive bone remodelling. *J Biomech* 15(3):141–154.
33. O'Connor JA, Lanyon LE, MacFie H (1982) The influence of strain rate on adaptive bone remodelling. *J Biomech* 15(10):767–781.
34. Raab DM, Crenshaw TD, Kimmel DB, Smith EL (1991) A histomorphometric study of cortical bone activity during increased weight-bearing exercise. *J Bone Miner Res* 6(7):741–749.
35. Kerschnitzki M, et al. (2013) Architecture of the osteocyte network correlates with bone material quality. *J Bone Miner Res* 28(8):1837–1845.
36. Dierckx P (1982) Algorithms for smoothing data with periodic and parametric splines. *Computer Graphics and Image Processing* 20(2):171–184.
37. Ramachandran P, Varoquaux G (2011) Mayavi- 3D visualization of scientific data. *Comput Sci Eng* 13(2):40–51.

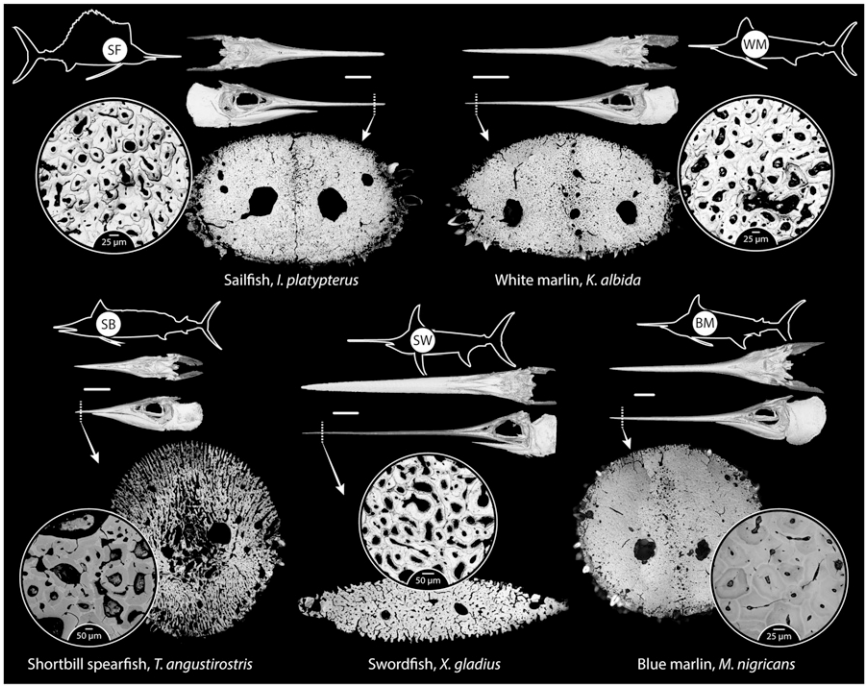

Fig. S1. Gross morphology and bone ultrastructure of the five billfish species examined in this study. For each species, the fish's body plan is shown as a silhouette, with CT scan images beneath showing the skull in dorsal and lateral perspectives. (Scale bars between CT scans: 10 cm.) Light microscopy images of distal, whole bill transverse cross-sections are shown beneath CT scans, demonstrating an array of complex ultrastructures, with circular inset images providing a higher magnification of the acellular osteonal tissue (backscatter electron images for the shortbill spearfish and blue marlin, and light microscopy images for all other species).